Proc. Natl. Acad. Sci. USA
Vol. 90, pp. 11089–11093, December 1993
Cell Biology

"BFA bodies": A subcompartment of the endoplasmic reticulum

(coatomer/Golgi/Sec23p/brefeldin)

LELIO ORCI*, ALAIN PERRELET*, MARIELLA RAVAZZOLA*, FELIX T. WIELAND†, RANDY SCHEKMAN‡, AND JAMES E. ROTHMAN§

*Department of Morphology, University of Geneva Medical School, 1211 Geneva 4, Switzerland; †Institute of Biochemistry I, University of Heidelberg, 6900 Heidelberg, Germany; ‡Division of Biochemistry and Molecular Biology, Howard Hughes Medical Institute, University of California, Berkeley, CA 94720; and §Program in Cellular Biochemistry and Biophysics, Rockefeller Research Laboratories, Sloan-Kettering Institute, New York, NY 10021

Contributed by Randy Schekman, August 9, 1993

ABSTRACT **A specialized region of the endoplasmic reticulum—the BFA body—is defined by the site of accumulation of coatomer when nonclathrin coat protein (COP)-coated vesicle assembly is prevented by the drug brefeldin A (BFA). BFA bodies are formed by part smooth, part rough domains of endoplasmic reticulum that are cis to the classical transitional endoplasmic reticulum and to BFA-induced Golgi remnants.**

Brefeldin A (BFA) has a profound effect on the structure of the Golgi apparatus (1–4), causing its normally stacked cisternal morphology to be converted into vesicular/cisternal remnants (5–8). In parallel with this structural alteration, resident Golgi membrane proteins typically redistribute to the endoplasmic reticulum (ER) via Golgi–ER "retrograde" membrane connections (9). Preceding these dramatic changes, ARF protein and coatomer [β-COP and other COPs (nonclathrin coat proteins)] dissociate from the Golgi membranes (10–12). We now report that BFA induces a reorganization of the ER–Golgi region resulting in the formation of an unusual structure—the BFA body—derived from modified ER cisternae.

MATERIAL AND METHODS

Tissue Preparation. Pancreatic islets of normal adult rats were isolated by collagenase digestion and incubated at 37°C under continuous shaking and gassing with 95% O_2/5% CO_2. Sets of islets were incubated in the presence of BFA (6 μg/ml) for 5–60 min. Samples were fixed with either 4% paraformaldehyde (immunofluorescence) or 1% glutaraldehyde buffered with 0.1 M sodium phosphate (electron microscopy) for 60 min at room temperature, washed with buffer, and processed for immunofluorescence after Epon embedding, or for cryoultramicrotomy according to Tokuyasu (13).

Immunocytochemistry. *Immunofluorescence.* Semithin sections (0.5–1 μm) of paraformaldehyde-fixed, Epon-embedded islet cells were collected on glass slides. Epon was removed according to Maxwell (14). After washing in distilled water, Epon-free sections were covered with a drop of anti-coatomer (β-COP) antibody (dilution, 1:100) for 120 min, washed in phosphate-buffered saline (PBS), and incubated with fluorescein isothiocyanate-conjugated goat anti-rabbit antiserum (dilution, 1:400) for 60 min. Sections were rinsed in PBS, counterstained with Evans blue, and photographed by fluorescence microscopy.

Electron microscopy. Frozen ultrathin sections were collected on nickel grids and processed by the protein A–gold technique (15). The sections were incubated for 60 min at room temperature with the respective primary antibodies, washed with PBS, and floated on a drop of protein A–gold solution (size of gold particles, 10 nm) for 30 min. After washing with distilled water, the sections were absorption-stained with uranyl acetate (16). The following primary antibodies and dilutions were used: rabbit anti-β-COP (EAGE antibody diluted 1:20, a gift from T. Kreis, European Molecular Biology Laboratory, Heidelberg), rabbit anti-β′-COP (C1-PL diluted 1:30), rabbit anti-γ-COP 768 (17) (diluted 1:10), rabbit anti-p20 (ξ-COP) (diluted 1:800), and rabbit anti-p36 (ε-COP) (diluted 1:400) (unpublished data). Anti-Sec23p antibody was used as described (18).

The quantitative evaluation of immunolabeling was performed on electron microscopic prints taken at a calibrated magnification. The cellular compartments were outlined with an electronic pen and the gold particles present on each compartment were recorded with the same pen connected to an IBM microprocessor programmed to calculate the number of gold particles per unit area/length.

RESULTS

Coatomer Distribution in Control Cells. At the immunofluorescence level, coatomer (β-COP) antibody elicits a reticular staining or a more concentrated perinuclear rim depending on the extension of the Golgi complex (Fig. 1*a*). At the ultrastructural level, the ER–Golgi configuration in the pancreatic β cell has been extensively described (19–21). By immunoelectron microscopy, coatomer immunoreactive sites are associated with the ER–Golgi transitional region and with the peripheral rim (cisternal tips and associated vesicles) of the Golgi complex (Fig. 1 *c* and *e*). The respective numbers of immunogold particles (β- and ε-COP) per unit length of membrane in the Golgi area are shown in Table 1. Sec23p immunoreactive sites are restricted to the transitional region (Fig. 1*d*).

Coatomer Distribution in BFA-Treated Cells. After 30 min of incubation of insulin cells in the presence of BFA, coatomer redistributes, now appearing condensed in discrete spots of variable sizes (Fig. 1*b*). At the ultrastructural level, the Golgi stack is converted to vesicular/cisternal remnants (5–8) that are surrounded by classical transitional regions (22) of the ER (Fig. 1*f*). In addition, a membrane compartment appears, which we term BFA bodies. The distinguishing features of BFA bodies are variously shaped cisternal profiles that are surrounded by a moderately dense cytosolic matrix (Figs. 1 *f* and *g* and 2). A close examination of the cisternal morphology in BFA bodies reveals that they consist of modified ER cisternae that are smooth on the side facing the dense matrix, while on the opposite side (in contact with the unmodified cytosol), they may bear ribosomes or may resemble unmodified transitional ER, having smooth protru-

The publication costs of this article were defrayed in part by page charge payment. This article must therefore be hereby marked "*advertisement*" in accordance with 18 U.S.C. §1734 solely to indicate this fact.

Abbreviations: ER, endoplasmic reticulum; COP, nonclathrin coat protein; BFA, brefeldin A.

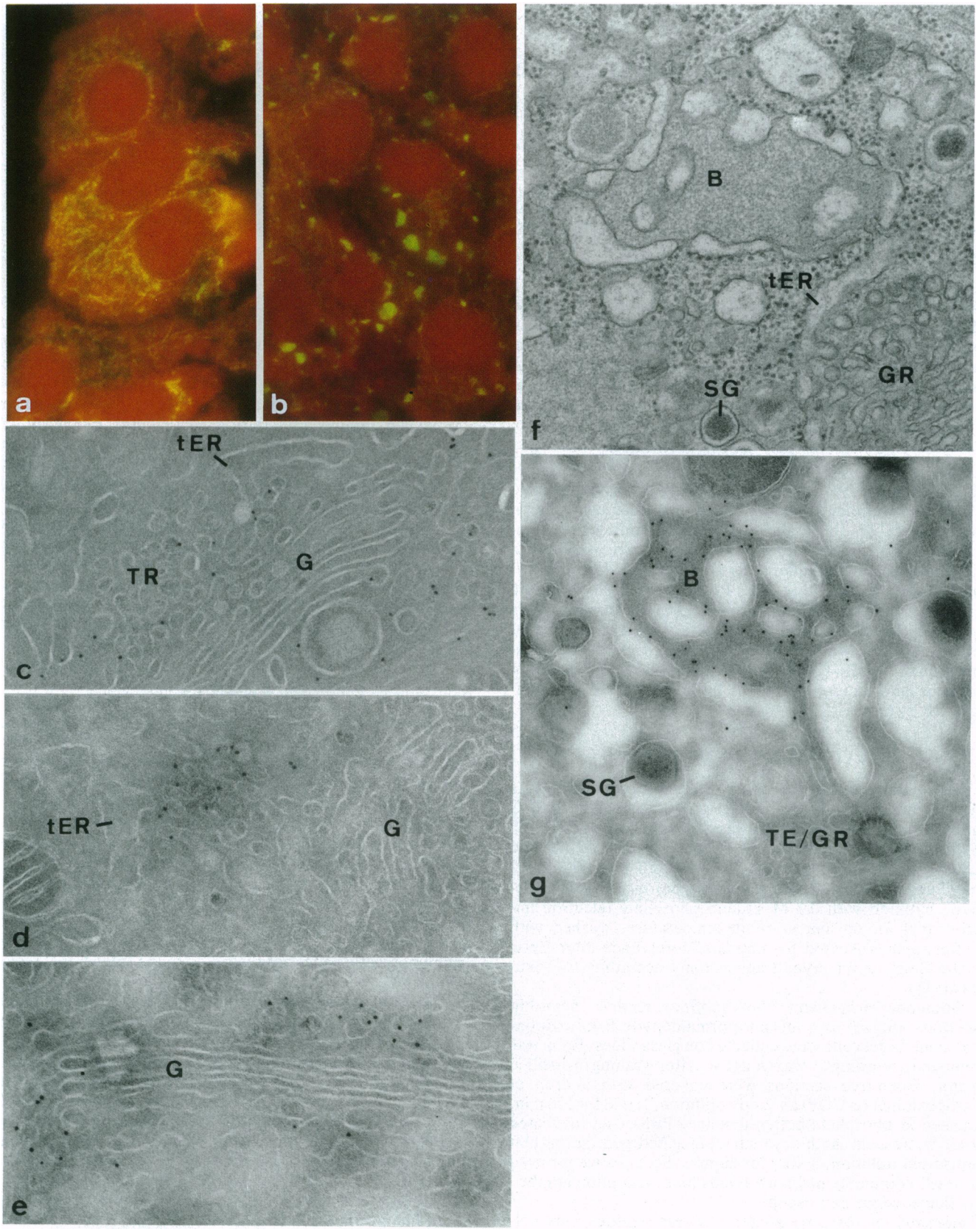

FIG. 1. (*a* and *b*) β-COP immunofluorescence on semithin sections. (*a*) Control insulin cells. Staining corresponding to the Golgi region can vary from a cytoplasmic reticular pattern to a more limited perinuclear staining. (*b*) BFA-treated insulin cells. Staining appears as discrete compact spots of various sizes. (*a* and *b*, ×1200.) (*c–e*) Golgi areas of untreated insulin cells. (*c*) β-COP immunogold particles appear over vesicular profiles in the transitional region (TR) and on vesicles present at the terminal rim of the Golgi stack (G). tER indicates a transitional cisterna with a smooth protrusion. See Table 1 for the quantitation of β-COP and p36 (ε-COP) immunolabeling. (×63,800.) (*d*) Sec23p immunogold labeling is restricted to the transitional region. The Golgi stack is unlabeled. (×74,900.) (*e*) p36 (ε-COP) immunogold particles label the transitional region and the terminal rim of the Golgi complex (G). Human insulin cell. (×63,000.) (*f* and *g*) BFA-treated insulin cells. (*f*) Conventional thin

Table 1. β-COP and ε-COP immunogold labeling per unit length (1 μm) of membrane in the Golgi region

	Buds and vesicles		
	Transitional region (including the smooth part of the transitional cisterna)	Golgi complex (lateral rim of cisterna and associated vesicles)	Golgi cisternae
β-COP	0.52 ± 0.09 (12 ± 3)	2.41 ± 0.35 (39 ± 4)	0.23 ± 0.06
ε-COP	1.03 ± 0.16 (24 ± 4)	3.78 ± 0.62 (55 ± 5)	0.55 ± 0.11

Shown in parentheses are percentages of vesicular profiles labeled. Background labeling was measured on the outer mitochondrial membrane: β-COP = 0.19 ± 0.05; ε-COP = 0.17 ± 0.06; *n* (number of pictures evaluated) = 15 for each antibody. The quantitation of coatomer immunolabeling in the Golgi region was carried out as follows. The smooth membrane of the transitional cisterna and of the associated buds and vesicles in the transitional region was outlined at a suitable magnification with an electronic pen to record their total length (in micrometers). The same operation was performed on the Golgi stack: the length of the terminal rim of the cisternae and the associated vesicles was measured as a single compartment; the length of the flat, uninterrupted portion of the stacked cisternae was recorded as a separate entity. Total immunogold particles present over these three respective compartments were counted and are expressed as numbers per unit length of membrane in the table.

sions and presumed transfer vesicles. BFA bodies can take a variety of shapes. Despite this, immunostaining by five different coatomer (23) antibodies—β-COP (24, 25), β′-COP (26), γ-COP (17), p20 (ξ-COP), and p36 (ε-COP) (unpublished data)—reveals the same pattern (Figs. 1*g* and 2): immunogold particles closely follow the geometry of the modified ER membranes that form the BFA bodies. Serial sectioning of the same BFA body reveals an exactly superimposable distribution of immunogold particles on each consecutive section (data not shown). Serial sectioning also reveals that BFA bodies are always intimately associated with typical transitional elements and Golgi remnants. Quantitative evaluation of the distribution of gold particles shows that >90% of the particles overlay or laterally touch the membranes, while <10% are seen at a distance over the surrounding condensed cytosol. BFA treatment does not appreciably alter the specific transitional regions of the ER, characterized by smooth protrusions and transfer vesicles. The specific Sec23p labeling of this area previously described in endocrine and acinar pancreatic cells (18) remains clearly detectable (see Fig. 1*d*), and there is a complete topographical segregation observable between the Sec23p labeling and that elicited by coatomer antibodies on BFA bodies (Fig. 2*d*). Even when a body is formed by only two (or three; see Fig. 2*a*) straight superimposed ER cisternae, with a transitional region separated by a fraction of a micrometer from the opposite, coatomer-labeled region, the transitional protrusions and transfer vesicles remain free of coatomer. Depletion of ATP with a variety of respiratory poisons also induced coatomer redistribution to these specialized regions of ER cisternae (data not shown). Under these conditions, however, the redistribution of coatomer is independent of Golgi disassembly.

DISCUSSION

We have reported a structure—the BFA body—that contains multiple subunits of coatomer. It is situated on the cis side of the classical transitional region and represents a subdivision of the ER. This is in keeping with the recent concept that the ER–Golgi pathway is composed of more distinct compartments [salvage compartment (27), intermediate compartment (28, 29), rubella virus accumulating compartment (30)] than envisioned when the transitional elements were originally described (22).

While it is widely assumed, based mainly on studies in cell-free systems with isolated Golgi membranes (11, 31), that coatomer is free in solution after BFA treatment, we report that in fact coatomer accumulates in living cells associated with a special membrane compartment—the BFA body. Indeed, within the BFA body, coatomer associates with a specialized domain of ER that is neither bulk ER nor transitional ER (marked by Sec23p).

While these data were being prepared for publication, two papers appeared describing the distribution of β-COP in pancreatic acinar cells treated with BFA or respiratory poisons (32, 33). Both papers report the formation of BFA-induced aggregates that stain with β-COP antibody (but not with Sec23p; ref. 32) and that associate with ER profiles morphologically distinct from the classical transitional protrusions. We rarely found such aggregates in insulin cells; BFA bodies were more apparent in cells that contain a more abundant ER cisternal component. Previous differences were noted, at the immunofluorescence level, in the distribution of β-COP after BFA-induced dissociation from Golgi membranes (10–12), and our observation might be another variation depending on the type of cell studied.

BFA is known to block the assembly of COP coats on Golgi membranes by inhibiting the activation of ARF protein by GTP–GDP exchange (34–37). Coatomer clearly associates with Golgi membrane (38) in a manner that is exclusively dependent on ARF (39–41). However, coatomer binding to ER membranes has not been studied and might involve additional interactions that may be ARF independent. Perhaps the sites of coatomer accumulation we report here are normally occupied only transiently, acting as a recruitment site from which ARF(GTP) can recruit coatomer for budding. When the level of ARF(GTP) is reduced by BFA, coatomer would accumulate at those sites to yield the changes observed. The peculiar shape and size of the BFA bodies should allow their isolation and biochemical characterization.

The persistence of budding profiles in the Sec23p-positive areas (i.e., transitional ER) in BFA bodies after coatomer depletion would seem to imply a coatomer-independent budding mechanism from transitional ER in the presence of BFA. However, because secretion is effectively stopped by BFA, any coatomer-independent pathway must be unproductive

section showing Golgi remnants (GR) surrounded by unmodified transitional elements (tER) of the endoplasmic reticulum. A BFA body (B) is formed by part rough, part smooth ER cisternae surrounding a homogeneous cytosolic matrix. The cisternal membrane in contact with the homogeneous matrix is smooth. SG, insulin secretory granule. (×42,000.) (*g*) Thin cryosection of a BFA body (B) immunostained with anti-β-COP antibody. Gold particles outline the side of the ER cisternal membranes facing the dense cytosolic matrix in the BFA body. Transitional elements/Golgi remnants (TE/GR) are unlabeled. (×50,700.)

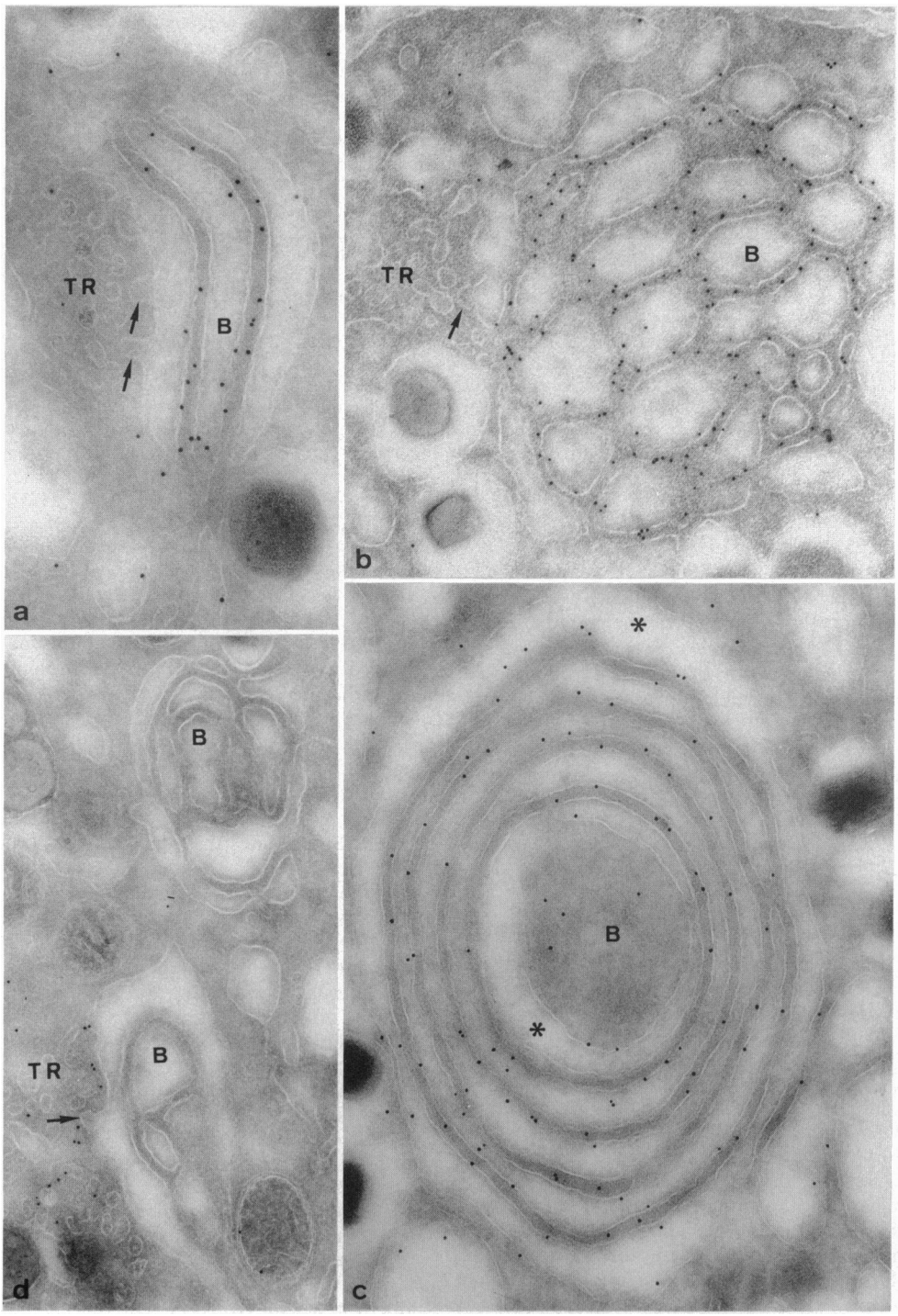

FIG. 2. (*a–d*) Thin cryosections of BFA bodies. (*a*) In this body, consisting of three superimposed ER cisternae (middle one is indicated by a B), the cisterna to the left has a typical transitional morphology (TR) on the outward face of the body. Arrows indicate transitional protuberances. Anti-p36 (ε-COP) immunostaining is absent from the transitional region but is associated with the cisternal membrane facing the condensed cytosol inside the body. The cisternal membrane in contact with the unmodified cytosol to the right is virtually unlabeled. (×59,200.) (*b*) BFA body formed by several circular ER profiles surrounding a dense matrix. One of the profiles is indicated by a B. Anti-p20 (ξ-COP) immunolabeling is restricted to the cisternal membrane facing the condensed cytosol. A typical transitional region (TR) is shown on the left, unstained by the coatomer antibody. Arrow indicates a smooth protuberance. (×41,200.) (*c*) BFA body formed by five concentric ER cisternae surrounding thin bands of condensed cytosol. Innermost and outermost cisternae of the BFA body are indicated by asterisks. β-COP immunolabeling is concentrated at the interface between the matrix and the membrane of the concentric cisternae, except on the innermost and outermost sides of the body. Both sides face an unmodified cytosol and are virtually unlabeled. (×43,500.) (*d*) Field of cytoplasm containing two BFA bodies (indicated by B). Lower body has a geometry comparable to that shown in *a*: one of its limiting cisternae has a typical transitional morphology (TR) on the outward side. Sec23p immunolabeling is restricted to the latter region, while both BFA bodies are unlabeled. Arrow indicates a transitional protrusion. (×40,500.)

relative to the coatomer-dependent pathway in living cells. Furthermore, studies in yeast have shown that coatomer and ARF are essential for protein transport from the ER (42, 43), although the precise role of coatomer in this limb of the yeast secretory pathway cannot be deduced from the genetic and cytologic experiments reported thus far. Our finding that

coatomer accumulates at sites adjacent to Sec23p is consistent with the idea that Sec23p and its associated proteins (Sar1p, Sec12p, and Sec24p; refs. 44 and 45) normally cooperate with the ARF coatomer system to produce COP-coated vesicles from the ER.

This work was supported by grants from the Swiss National Science Foundation (L.O.), the Human Frontier Science Program (J.E.R., F.T.W., and L.O.), and the Howard Hughes Medical Institute (R.S.).

1. Misumi, Y., Miki, A., Takatsuki, A., Tamura, G. & Ikehara, Y. (1986) *J. Biol. Chem.* **261,** 11398–11403.
2. Oda, K., Hirose, S., Takami, N., Misumi, A., Takatsuki, A. & Ikehara, Y. (1987) *FEBS Lett.* **214,** 135–138.
3. Fujiwara, T., Oda, K., Yokota, S., Takatsuki, A. & Ikehara, Y. (1988) *J. Biol. Chem.* **263,** 18545–18552.
4. Lippincott-Schwartz, J., Yuan, L. C., Bonifacino, J. S. & Klausner, R. D. (1989) *Cell* **56,** 801–813.
5. Hendricks, L. C., McClanahan, S. L., McCaffery, M., Palade, G. E. & Farquhar, M. G. (1992) *Eur. J. Cell Biol.* **58,** 202–213.
6. De Lemos-Chiarandini, C., Ivessa, N. E., Black, V. H., Tsao, Y. S., Gumper, I. & Kreibich, G. (1992) *Eur. J. Cell Biol.* **58,** 187–201.
7. Hidalgo, J., Garcia-Navarro, R., Garcia-Navarro, F., Perez-Vilar, J. & Velasco, A. (1992) *Eur. J. Cell Biol.* **58,** 214–227.
8. Sandvig, K., Prydz, K., Hansen, S. H. & Van Deurs, B. (1991) *J. Cell Biol.* **115,** 971–981.
9. Lippincott-Schwartz, J., Donaldson, J. G., Schweizer, A., Berger, E. G., Hauri, H.-P., Yuan, L. C. & Klausner, R. D. (1990) *Cell* **60,** 821–836.
10. Donaldson, J. G., Lippincott-Schwartz, J., Bloom, G. S., Kreis, T. & Klausner, R. D. (1990) *J. Cell Biol.* **111,** 2295–2306.
11. Orci, L., Tagaya, M., Amherdt, M., Perrelet, A., Donaldson, J. G., Lippincott-Schwartz, J., Klausner, R. D. & Rothman, J. E. (1991) *Cell* **64,** 1183–1195.
12. Robinson, M. S. & Kreis, T. E. (1992) *Cell* **69,** 129–138.
13. Tokuyasu, K. T. (1980) *Histochem. J.* **12,** 381–403.
14. Maxwell, M. H. (1978) *J. Microsc. (Oxford)* **112,** 253–255.
15. Roth, J., Bendayan, M. & Orci, L. (1978) *J. Histochem. Cytochem.* **26,** 1074–1081.
16. Tokuyasu, K. T. (1986) *J. Microsc. (Oxford)* **143,** 139–149.
17. Stenbeck, G., Schreiner, R., Herrmann, D., Auerbach, S., Lottspeich, F., Rothman, J. E. & Wieland, F. T. (1992) *FEBS Lett.* **314,** 195–198.
18. Orci, L., Ravazzola, M., Meda, P., Holcomb, C., Moore, H.-P., Hicke, L. & Schekman, R. (1991) *Proc. Natl. Acad. Sci. USA* **88,** 8611–8615.
19. Orci, L. (1974) *Diabetologia* **10,** 163–187.
20. Orci, L. (1982) *Diabetes* **31,** 538–565.
21. Orci, L., Ravazzola, M., Amherdt, M., Louvard, D. & Perrelet, A. (1985) *Proc. Natl. Acad. Sci. USA* **82,** 5385–5389.
22. Palade, G. E. (1975) *Science* **189,** 347–358.
23. Waters, M. G., Serafini, T. & Rothman, J. E. (1991) *Nature (London)* **349,** 248–251.
24. Duden, R., Griffiths, G., Frank, R., Argos, P. & Kreis, T. E. (1991) *Cell* **64,** 649–665.
25. Serafini, T., Stenbeck, G., Brecht, A., Lottspeich, F., Orci, L., Rothman, J. E. & Wieland, F. T. (1991) *Nature (London)* **349,** 215–220.
26. Stenbeck, G., Harter, C., Brecht, A., Herrmann, D., Lottspeich, F., Orci, L. & Wieland, F. T. (1993) *EMBO J.* **12,** 2841–2845.
27. Pelham, H. R. B. (1991) *Curr. Opin. Cell Biol.* **3,** 585–591.
28. Schweizer, A., Franzen, J. A. M., Matter, K., Kries, T. E. & Ginsel, G. (1990) *Eur. J. Cell Biol.* **53,** 185–196.
29. Schweizer, A., Matter, K., Ketcham, C. M. & Hauri, H. P. (1991) *J. Cell Biol.* **113,** 45–54.
30. Hobman, T. C., Woodward, L. & Farquhar, M. G. (1992) *J. Cell Biol.* **118,** 795–812.
31. Klausner, R. D., Donaldson, J. G. & Lippincott-Schwartz, J. (1992) *J. Cell Biol.* **116,** 1071–1080.
32. Oprins, A., Duden, R., Kreis, T. E., Geuze, H. J. & Slot, J. W. (1993) *J. Cell Biol.* **121,** 49–59.
33. Hendricks, L. C., McCaffery, M., Palade, G. E. & Farquhar, M. G. (1993) *Mol. Biol. Cell* **4,** 413–424.
34. Donaldson, J. G., Finazzi, D. & Klausner, R. D. (1992) *Nature (London)* **360,** 350–352.
35. Helms, J. B. & Rothman, J. E. (1992) *Nature (London)* **360,** 352–354.
36. Donaldson, J. G., Cassel, D., Kahn, R. A. & Klausner, R. D. (1992) *Proc. Natl. Acad. Sci. USA* **89,** 6408–6412.
37. Serafini, T., Orci, L., Amherdt, M., Brunner, M., Kahn, R. A. & Rothman, J. E. (1991) *Cell* **67,** 239–253.
38. Orci, L., Palmer, D. J., Ravazzola, M., Perrelet, A., Amherdt, M. & Rothman, J. E. (1993) *Nature (London)* **362,** 648–652.
39. Orci, L., Palmer, D. J., Amherdt, M. & Rothman, J. E. (1993) *Nature (London)* **364,** 732–734.
40. Kahn, R. A., Randazzo, P., Serafini, T., Weiss, O., Rulka, C., Clark, J., Amherdt, M., Roller, P., Orci, L. & Rothman, J. E. (1992) *J. Biol. Chem.* **267,** 13039–13046.
41. Palmer, D. J., Helms, J. B., Beckers, C. J. M., Orci, L. & Rothman, J. E. (1993) *J. Biol. Chem.* **268,** 12083–12089.
42. Hosobuchi, M., Kreis, T. & Schekman, R. (1992) *Nature (London)* **360,** 603–605.
43. Stearns, T., Willingham, M., Botstein, D. & Kahn, R. (1990) *Proc. Natl. Acad. Sci. USA* **87,** 1238–1242.
44. Yoshihisa, T., Barlowe, C. & Schekman, R. (1993) *Science* **259,** 1466–1468.
45. Barlowe, C. & Schekman, R. (1993) *Nature (London)* **365,** 347–349.